Hybrid lipids increase nanoscale fluctuation lifetimes in mixed membranes

Benoit Palmieri and Samuel A. Safran*

Department of Materials and Interfaces, Weizmann Institute of Science, Rehovot 76100, Israel

(Received 12 May 2013; revised manuscript received 22 August 2013; published 10 September 2013)

A recently proposed ternary mixture model is used to predict fluctuation domain lifetimes in the one phase region. The membrane is made of saturated, unsaturated, and hybrid lipids that have one saturated and one unsaturated hydrocarbon chain. The hybrid lipid is a natural linactant which can reduce the packing incompatibility between saturated and unsaturated lipids. The fluctuation lifetimes are predicted as a function of the hybrid lipid fraction and the fluctuation domain size. These lifetimes can be increased by up to three orders of magnitude compared to the case of no hybrids. With hybrid, small length scale fluctuations have sizable amplitudes even close to the critical temperature and, hence, benefit from enhanced critical slowing down. The increase in lifetime is particularly important for nanometer scale fluctuation domains where the hybrid orientation and the other lipids composition are highly coupled.

DOI: 10.1103/PhysRevE.88.032708 PACS number(s): 87.16.dj, 87.14.Cc, 87.15.Zg, 87.16.dt

I. INTRODUCTION

The recent discovery that cell membranes contain nanodomains of uniform composition (lipid "rafts") that are believed to mediate cellular function [1–9] has motivated numerous experiments on model systems. The study of self-assembled giant unilamelar vesicles (GUVs) whose composition (i.e., lipids, cholesterol) can be controlled [10–16] or extracted from cell membranes [10,17,18] provides useful information regarding the interactions among membrane constituents since they are not subject to other types of interactions present in real cells (i.e., coupling with the cytoskeleton and/or active processes).

Recent experiments on GUVs assembled from cell membrane extracts [17] reported critical composition fluctuations that are consistent with scaling laws [19] of the two-dimensional (2D) Ising model with a critical temperature of $T_c \approx 23\,^{\circ}\mathrm{C}$. The large fluctuation domain sizes observed close to T_c were extrapolated to $T = 37\,^{\circ}\mathrm{C}$ (physiological temperature) and predicted a correlation length of $\xi \approx 20$ nm, which is of the order of estimated raft sizes. At such a temperature ($\approx$5% above T_c), fluctuation domains of 20 nm can be shown to have lifetimes of the order of $\tau \approx 1$ ms. This will be shown later using the scaling laws of model B [20,21] and assuming small fluctuation amplitudes (Gaussian fluctuations). It has recently been proposed that some biochemical reactions can be facilitated by rafts with $<$0.1 ms lifetime [22], but those that are believed to participate in cell signaling are expected to be stable over several minutes [23]. This does not eliminate the possibility that the mechanism for lipid raft stabilization may benefit from the fact that real cell membranes are close enough to a miscibility critical point. In fact, in real cells, the phase behavior may be significantly coupled to hydrodynamic modes [21,24], the cytoskeleton [25], and/or membrane proteins [23,26–28]. Using a continuum description of the single phase regime, we show how fluctuation lifetimes are strongly dependent on the membrane composition. In particular, a simple ternary mixture model membrane made of saturated, unsaturated, and line active "hybrid" lipids predicts that nanoscale composition fluctuations can have a much larger lifetime compared to the case with no hybrids.

The model was introduced in a recent paper [29]. It assumes that the phase separation is driven by the chain packing incompatibility between "straight" saturated and "bent" unsaturated hydrocarbon chains. The permanent bend is due to the presence of one or more double bonds in the chain. Our hypothesis is that hybrid lipids can reduce the line tension when they assemble at a saturated-unsaturated interface with the proper orientation [see Fig. 1(a)]; the hybrid lipid has one chain of both types and it can act as a linactant (2D analog of a surfactant) [30]. The phase separation in model membranes made of saturated, unsaturated, and hybrid lipids has been studied experimentally in Refs. [15,31,32]. Such systems can be described by our model and some comparisons between theory and experiments were presented in [29]. Note that real cell membranes contain numerous types of saturated and hybrid lipids, but almost no unsaturated lipids. Nevertheless, our model could be used to describe real cell membranes since one subclass of hybrid lipids may effectively behave as unsaturated lipids with respect to packing compatibility with other subclasses of hybrid and saturated lipids.

Other models based on the coupling between membrane curvature [33–35] and/or membrane elastic properties [36] with the lipid phase separation have been proposed as possible mechanisms for the formation of small domains in model membranes. Such effects are not included in our model since they would obscure our main objective, which is to demonstrate that the interplay between the hybrid orientation degrees of freedom and the membrane composition *alone* can increase the dynamical stability of composition fluctuations.

In Ref. [29], we focused on the static properties of membranes in the single phase and showed that at relatively large hybrid fractions, nanoscale fluctuation domains can be observed *even if the temperature is close to the critical temperature*. Small length scale fluctuations have sizable amplitudes even close to the critical temperature, where large correlation lengths are usually expected.

Our continuum theory extends the lattice model proposed by Matsen and Sullivan [37], the continuum model of Hirose *et al.* [38], and other early microemulsion models [39,40].

*Corresponding author.

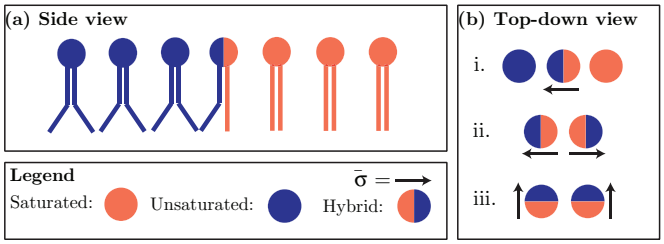

FIG. 1. (Color online) (a) Example of how hybrid lipids can reduce the packing incompatibility between saturated and unsaturated lipids. (b) Examples of local lipid configurations that minimize (i) $\mathcal{E}_{\phi\sigma}$, (ii) first term of $\mathcal{E}_{\sigma\sigma}$, and (iii) second term of $\mathcal{E}_{\sigma\sigma}$ in Eqs. (2.1) and (2.2).

The unique features of our model are that it contains a single parameter (specified by the demixing temperature) and that the composition dependence of the system is fully taken into account. The latter will allow us to predict how the fluctuation dynamical properties vary as hybrid lipids are added to the membrane. Hirose *et al.* [38] reported the dynamic structure factors of composition fluctuations for a system with hybrids using a phenomenological approach in which the hybrid composition is not explicitly taken into account. They further assumed that the lipid reorientation occurs on a much shorter time scale than the lipid lateral diffusion. We will show that this is not necessarily true for nanoscale fluctuations.

Considering fluctuation domains of a given size, we predict the dependence of their lifetimes on the hybrid lipids fraction. The results are as follows: (i) With increasing hybrid fractions, the amplitude of small length scale ($\approx$10 nm) fluctuations is relatively large even near T_c; critical slowing down affects even small length scale fluctuations. (ii) The smaller the fluctuation length scale, the larger the coupling between orientation fluctuations of the hybrids and the composition fluctuations of the other lipids. Combined, these effects predict that the lifetime of fluctuations of all length scales, including the nanoscale relevant to lipid rafts, can increase by orders of magnitude in a temperature range of the order of 10 °C above T_c, which is easily accessible experimentally.

Please note that the main body of the paper focuses on the physics and that all mathematical details are presented in the Appendices.

II. RESULTS AND DISCUSSION

A. Review of static properties

This section reviews some of the results we obtained in [29], which set the stage for the analysis of the fluctuation lifetimes. The model extends previous ones proposed by Brewster *et al.* [41] and Yamamoto *et al.* [42,43] by including the orientation degrees of freedom of the hybrid lipid. In [29], the following coarse-grained theory for the mixed phase fluctuation free energy is derived from a reduced set of nearest-neighbor chain-chain interactions,

$$\mathcal{F}_{\text{Fluct}} = \mathcal{E}_{\phi\phi} + \mathcal{E}_{\phi\sigma} + \mathcal{E}_{\sigma\sigma} - T\mathcal{S}, \tag{2.1}$$

where T is the temperature, $\mathcal{S}$ is the entropy of the fluctuations, and $\mathcal{E}_{m,n}$ describes the interaction energies due to saturated-unsaturated-hybrid composition ($m,n = \phi$) and hybrid orientation ($m,n = \sigma$) fluctuations. A full expression for the entropic free-energy cost associated with local fluctuations is reported in Eq. (A3). It depends explicitly on the average membrane fraction of saturated, unsaturated, and hybrid lipids ($\phi_s^{(0)}$, $\phi_u^{(0)}$, and $\phi_h^{(0)} = 1 - \phi_s^{(0)} - \phi_u^{(0)}$) and it is a quadratic function of the local saturated (unsaturated) lipid composition fluctuations $[\delta\phi_{s[u]}(\mathbf{x})]$ and of the local hybrid lipid orientation fluctuation vector $[\bar{\sigma}(\mathbf{x}) = \hat{x}\sigma_x(\mathbf{x}) + \hat{y}\sigma_y(\mathbf{x})$; not to be confused with lipid tilting, which is not included in our model]. The composition fluctuations are defined as a local deviation from the membrane average; $\delta\phi_{s[u]}(\mathbf{x}) = \phi_{s[u]}(\mathbf{x}) - \phi_{s[u]}^{(0)}$ [$\delta\phi_h(\mathbf{x}) = -\delta\phi_s(\mathbf{x}) - \delta\phi_u(\mathbf{x})$ by conservation of mass]. Note that $\bar{\sigma}(\mathbf{x})$ [like $\phi_{s,u,h}(\mathbf{x})$] is a coarse-grained degree of freedom and, hence, it assumes continuous values (in contrast to the lattice model orientation unit vector from which it originates; see Ref. [29]).

The complete expressions for the interaction terms are given in Eqs. (A4)–(A7). For illustration purposes, we report them to second order in a gradient expansion,

$$\begin{aligned}
\mathcal{E}_{\phi\phi} &\approx -\frac{2J}{a^2}\int d\mathbf{x}\left[\Psi(\mathbf{x})^2 - \frac{a^2}{4}|\nabla\Psi(\mathbf{x})|^2\right],\\
\mathcal{E}_{\phi\sigma} &\approx \frac{2J}{a^2}\int d\mathbf{x}\left[\frac{a}{2}\bar{\sigma}(\mathbf{x})\cdot\nabla\Psi(\mathbf{x})\right],\\
\mathcal{E}_{\sigma\sigma} &\approx -\frac{2J}{a^2}\int d\mathbf{x}\left[\frac{a^2}{8}|\nabla\cdot\bar{\sigma}(\mathbf{x})|^2 - \frac{a^2}{8}|\nabla\times\bar{\sigma}(\mathbf{x})|^2\right],
\end{aligned} \tag{2.2}$$

where $\Psi(\mathbf{x}) = \delta\phi_s(\mathbf{x}) - \delta\phi_u(\mathbf{x})$, a is a molecular size, and J is the interaction parameter. The term $\mathcal{E}_{\phi\phi}$ accounts for saturated-unsaturated composition interactions. It favors (is negative for) saturated and unsaturated lipids phase separation. The term $\mathcal{E}_{\phi\sigma}$ is a composition-orientation interaction that favors local interactions such as the one illustrated in Fig. 1(b)(i). *The line active property of the hybrids is due to that interaction term* [note that in Fig. 1(b)(i), if the hybrid had the opposite orientation, the line tension would not be reduced]. $\mathcal{E}_{\sigma\sigma}$ are hybrid lipid orientation-orientation interaction terms that favor orientation fluctuations that change sign on the smallest length scale, a, in the direction parallel to the local orientation vector [first term of $\mathcal{E}_{\sigma\sigma}$ and Fig. 1(b)(ii)] or that favors uniform orientation fluctuations in the direction perpendicular to the local orientation vector [second term of $\mathcal{E}_{\sigma\sigma}$ and Fig. 1(b)(iii)].

Reference [29] showed that a line of critical points is found along $\phi_s^{(0)} = \phi_u^{(0)}$ and $\phi_h^{(0)} < 2/3$ such that

$$T_c = 4J\left(1 - \phi_h^{(0)}\right). \tag{2.3}$$

This indicates that the hybrids decrease T_c (increase the stability of the mixed state) and shows the one-to-one correspondence between the system parameter J and the demixing temperature. Because we want to analyze the lifetime of critical fluctuations, we restrict ourselves to $\phi_s^{(0)} = \phi_u^{(0)}$ and $\phi_h^{(0)} < 2/3$. Note that $\phi_h^{(0)} = 2/3$ defines a Lifshitz point above which anisotropic "stripelike" fluctuations dominate the uniform and isotropic fluctuations. These are discussed in detail in Ref. [29] and are due to the $\mathcal{E}_{\sigma\sigma}$ terms.

One main prediction made in [29] is that the correlation length ξ of lipid composition fluctuations ("domain size") decreases significantly as the fraction of hybrids increases toward the Lifshitz point. A full expression for ξ is given

by Eq. (A16) and reduces to

$$\left(\frac{\xi}{a}\right)^2 = \theta^{-1}\left[\frac{1-3\phi_h^{(0)}/2}{4\left(1-\phi_h^{(0)}\right)}\right], \tag{2.4}$$

when $\phi_h^{(0)} < 2/3$ and $\theta = (T - T_c)/T_c \ll 1$. As expected in a mean-field approximation, ξ/a diverges as $\theta^{-1/2}$ as the critical temperature is approached as long as $\phi_h^{(0)} < 2/3$. Exactly at the Lifshitz line ($\phi_h^{(0)} = 2/3$), a different scaling law is obtained, $\xi/a \propto \theta^{-1/4}$ as $\theta \to 0$ (see Appendix A or Chap. 4.6 in Ref. [44]). Here, we restrict our attention to $\phi_h^{(0)} < 2/3$ and do not consider the Lifshitz point.

B. Dynamical predictions

The composition fluctuations of each species are conserved [the membrane average of $\delta\phi_{s,u}(\mathbf{x})$ vanishes]. Hence, the simplest dynamics that describes their time dependence is

$$\frac{\partial\delta\phi_{s,u}(\mathbf{x})}{\partial t} = D_0\nabla^2\frac{\mathcal{D}\mathcal{F}_{\text{Fluct}}}{\mathcal{D}\delta\phi_{s,u}(\mathbf{x})}, \tag{2.5}$$

where D_0 is related to the lipid diffusion coefficient, D ($D_0 = a^2D/T$), and $\mathcal{D}$ is a functional derivative. The orientations are not conserved so their dynamics can be described by a relaxation equation,

$$\frac{\partial\sigma_{x,y}(\mathbf{x})}{\partial t} = -\Gamma\frac{\mathcal{D}\mathcal{F}_{\text{Fluct}}}{\mathcal{D}\sigma_{x,y}(\mathbf{x})}, \tag{2.6}$$

where Γ is related to the reorientation time scale γ^{-1} ($\Gamma = \gamma a^2/T$). It determines the time a hybrid takes to change its local orientation due to fluctuations. This set of dynamical equations is in the class of model C defined in Ref. [20] (or Sec. 8.6 of Ref. [44]), where it is also shown how thermal noise can be included. Note that with no hybrids, the system of dynamical equations reduces to model B.

The role of the hybrid orientation degrees of freedom on the composition fluctuation dynamics depends on a dimensionless parameter, $\eta = \tau_0/\gamma^{-1}$ (see Appendix B), which is the ratio of the time scale for a lipid to diffuse over a distance equal to its own size, $\tau_0 = a^2/D$, to the reorientation time scale γ^{-1}. Honigmann *et al.* [45] reported $D \approx 20\ \mu\text{m}^2/\text{s}$ and $\gamma \approx 10^8\ \text{s}^{-1}$ for various fully saturated lipid probes in a model membrane made of saturated and unsaturated lipids and cholesterol. Taking their values with $a \approx 0.5$ nm gives $\eta \approx 1$. Thus, *the diffusion and reorientation time scales are of the same order*. Others [17,46–48] have reported slightly different D and γ for different lipid probes or lipid analogs. We also expect the characteristic time scales of unsaturated lipids to exceed those of the saturated lipids probes used in [45]. Hence, we assume that physically relevant values for η lie in a range close to $\eta = 1$.

Insight into the dynamic stability of fluctuation domains of *fixed* length scales in the presence of hybrid lipids can be obtained from the following analysis. We consider a fluctuation in the single phase of the form

$$\bar{\Psi}(x) = \bar{\Psi}^{(a)}\cos(2\pi x/\lambda) + \bar{\Psi}^{(b)}\sin(2\pi x/\lambda), \tag{2.7}$$

where $\bar{\Psi}(x) = [\delta\phi_s(x),\delta\phi_u(x),\sigma_x(x),\sigma_y(x)]$ is a one-dimensional array containing the composition and orientation fluctuations. $\bar{\Psi}^a$ and $\bar{\Psi}^b$ are arrays containing the fluctuation amplitudes. The fact that the system is rotationally invariant allows us to arbitrarily set $\mathbf{x} = x\hat{x}$ (no components along $\hat{y}$) with no loss of generality. Equation (2.7) is inserted in Eqs. (2.5) and (2.6) to obtain the lifetime of such a fluctuation. The procedure is detailed in Appendix B where an exact expression for the mode with the longest lifetime [Eq. (B4)] is reported. The nonzero components of the fluctuation amplitude, $\bar{\Psi}^{(a)}$ and $\bar{\Psi}^{(b)}$, are $\delta\phi_s^{(a)}$, $\delta\phi_u^{(a)}$ (in fact, $\delta\phi_s^{(a)} = \delta\phi_u^{(a)}$), and $\sigma_x^{(b)}$. For that mode, this implies that (i) $\phi_{s(u)}(x)$ are out of phase with $\sigma_x(x)$ such that the hybrid lipid orientation fluctuation is maximized (strongly correlated) at the interface between fluctuation domains rich in either saturated or unsaturated lipids, and (ii) the hybrid lipid composition does not fluctuate ($\delta\phi_h^{(a)} = 0$).

For long fluctuation wavelengths $\lambda \gg a$, small reduced temperatures $\theta \ll 1$, and small $\eta \ll 1$, the lifetime reported in Eq. (B4) simplifies to

$$\frac{\tau\left(\theta,\phi_h^{(0)}\right)}{\tau_0} \approx \left\{\frac{4\theta}{\tilde{\lambda}^2} + \frac{1-\frac{3\phi_h^{(0)}}{2}}{\tilde{\lambda}^4\left(1-\phi_h^{(0)}\right)} - \tau_\eta\left(\theta,\phi_h^{(0)}\right)\right\}^{-1}, \tag{2.8}$$

where

$$\tau_\eta\left(\theta,\phi_h^{(0)}\right) = \frac{{\phi_h^{(0)}}^2\theta}{2\eta\tilde{\lambda}^6\left(1-\phi_h^{(0)}\right)^2}, \tag{2.9}$$

and $\tilde{\lambda} = \lambda/2\pi a$. The second term on the right-hand side of Eq. (2.8) shows that the lifetime increases as the hybrid fraction is increased toward the Lifshitz point. For long wavelength fluctuations, the dimensionless parameter η (the ratio of the diffusion timescale to the reorientation timescale) has only small effects, as can be seen from Eq. (2.9). This is expected because local reorientation is much faster than the diffusion over large length scales. In such a case, $\tilde{\lambda} \gg 1$ and the separation of time scales approximation used by Hirose *et al.* [38] is appropriate. On the other hand, Eq. (2.9) shows that the effect of η becomes increasingly important for smaller values of η, smaller fluctuation domains, and larger hybrid fractions. Note that for a system with no hybrids, Eq. (2.8) predicts that a 20 nm fluctuation at $\theta = 0.01$–0.05 will have a lifetime $\tau \approx 1$ ms, as stated in Sec. I. The 20 nm scale is the correlation length extrapolated at $T = 37\,^\circ$C from the lower temperature measurements in Ref. [17].

Figure 2 reports $\tau(\theta,\phi_h^{(0)})$ vs θ for various length scales and hybrid fractions. The results demonstrate that (a) for $\lambda = 40a$ ($\approx$20 nm), critical slowing down manifests itself as far as 5% above T_c. The θ axis translates into a 3–15 K range for typical T_c values and is easily accessible experimentally. In fact, the lifetime of such fluctuations reaches the millisecond range not too close to T_c and at moderate hybrid fractions. (b) Small length scale ($\lambda = 10a$) fluctuations have a smaller fluctuation lifetime than larger length scale fluctuations. On the other hand, the relative increase in lifetime due to hybrids at small length scales is much larger; it can reach 1–2 orders of magnitude and increases when η decreases (saturated and unsaturated fluctuation domains are stabilized by slow orientation fluctuations correlated with their interface).

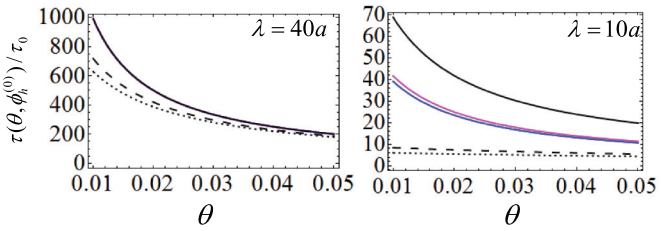

FIG. 2. (Color online) The lifetime of a fluctuation of the form of Eq. (2.7) with $\lambda = 40a$ (left) and $\lambda = 10a$ (right) as a function of the reduced temperature θ. In each panel, the bottom (short dashes) curves are for $\phi_h^{(0)} = 0.01$, the middle (large dashes) curves are for $\phi_h^{(0)} = 0.4$, and the top (full line) curves are for $\phi_h^{(0)} = 0.66$ (close to the Lifshitz point). For $\lambda = 40a$, the lifetimes are insensitive to the parameter η. Effects of η are clearly observed for $\lambda = 10a$ and $\phi_h^{(0)} = 0.66$ where the blue (bottom), magenta (middle), and black (top) curves were obtained using $\eta = 10$, 1, and 0.1, respectively. The lifetime is reported in units of $\tau_0 = a^2/D \approx 10^{-6}$–$10^{-7}$ s.

At a given temperature, not all fluctuation domain sizes are equally probable. Hence, it gives more physical insight to focus on fluctuation domains with the characteristic size (i.e., root mean squared average size). This is what we do next by setting the fluctuation length scale λ equal to the correlation length ξ. Hence, we set $\lambda = \xi$ in Eq. (2.7) and recalculate the lifetime $\tau(\xi,\phi_h^{(0)})$ and the fluctuation amplitudes $\bar{\Psi}^{(a,b)}$. The temperature θ depends implicitly on the values of the hybrid fraction and the correlation length [Eqs. (2.4), (A16), and Fig. 4 show how close one must be to T_c to observe a given ξ].

The lifetime $\tau(\xi,\phi_h^{(0)})$ is shown in Fig. 3 as a function of the hybrid fraction for $\xi/a = 10$ and $\xi/a = 4$ and for $\eta = 0.1$ (which gave the largest lifetimes in Fig. 2). It increases smoothly by about two orders of magnitude as the hybrid lipid fraction approaches the Lifshitz point. For $\xi/a = 10$, this large increase in lifetime only occurs very close to the Lifshitz point (as $\phi_h^{(0)} \to 2/3$). On the other hand, for $\xi/a = 4$, a significant increase (one order of magnitude) is observed even at moderate hybrid fractions ($\phi_h^{(0)} \approx 0.3$–0.4). Appendix B shows that as the hybrid composition approaches the Lifshitz point ($\phi_h^{(0)} \approx 2/3$), the increase in long wavelength ($\xi \gg a$) fluctuation lifetime due to hybrids scales with the following power law: $\tau(\xi,\phi_h^{(0)})/\tau(\xi,\phi_h^{(0)} = 0) \propto (\xi/a)^2$.

The insets in Fig. 3 show a measure, $\kappa^2 = \sigma_x^{(b)2}/(\delta\phi_s^{(a)2} + \delta\phi_u^{(a)2})$, of the coupling between orientation and composition fluctuations. As the hybrid fraction increases, κ increases significantly. The physical origin of the increased lifetime is directly related to the orientation fluctuations that stabilize the interface region between saturated and unsaturated rich fluctuation domains [29]. For $\xi/a = 4$, a significant coupling between composition and orientation fluctuations is observed at lower hybrid fractions compared to $\xi/a = 10$. This is consistent with Eqs. (2.2) and (A5) [illustrated in Fig. 1(b)(i)], which show that the coupling between orientation and composition fluctuations is stronger at small wavelengths. Experiments confirming that hybrid lipids are orientationally correlated with the composition gradient at the interface remain to be done, but recent molecular dynamics studies with realistic force fields support this hypothesis [49].

III. CONCLUDING REMARKS

In summary, we have shown that with increasing hybrid fraction, the reduced temperature that corresponds to a given correlation length is smaller. Hence, critical slowing down has larger effects in systems with hybrids and longer lifetimes are predicted. Moreover, the predicted increase in lifetime occurs in a broad region above T_c (as large as 15 K; see Fig. 2). Of course, our analysis is not appropriate for large amplitude fluctuations *very* close to the critical point. In this case, model B (applied to 2D membranes) predicts that $\tau \propto \theta^{-3.75}$ [20], while our Gaussian fluctuation analysis predicts $t \propto \theta^{-2}$ (this can be seen by replacing $\tilde{\lambda}$ in Eq. (2.8) by the mean-field correlation length given in Eq. (2.4)). Nevertheless, we expect that the effect demonstrated here, i.e., an increase in fluctuation lifetime due to hybrids, will manifest itself regardless of the scaling law as long as the correlation length is small enough.

The predicted effect on the lifetime is particularly important for fluctuating nanodomains where the hybrid orientation and composition degrees of freedom are highly coupled and where the reorientation time scale of the hybrids can be of the order (perhaps even longer) of the time scale for the diffusion over one molecular size: $\eta \leqslant 1$. This contrasts with the experiment of Honerkamp-Smith *et al.* [21] (inspired by the theoretical proposition made in Refs. [50,51]), who showed how coupling the hydrodynamics modes in the membrane with those of the surrounding solvent can also increase composition fluctuation lifetimes. They report that the scaling law for the lifetime crosses over from $\tau \propto \theta^{-2}$ to $\tau \propto \theta^{-3}$ when the correlation length is in the 1–5 μm range. Interestingly, the $\tau \propto \theta^{-2}$ scaling law observed for the smaller correlation lengths studied in their experiment agrees with our Gaussian fluctuation analysis, although their claim is that this arises when the hydrodynamics of the bulk solvent plays a negligible role compared with the hydrodynamics of the membrane itself.

Finally, note that the two mechanisms are not mutually exclusive: the hydrodynamic effects are important at much larger length scales compared with the effect we predict, which becomes important at smaller length scales (≈10 nm). We hope that further dynamical experiments that measure the time scales that determine η as well as the dynamic structure factor

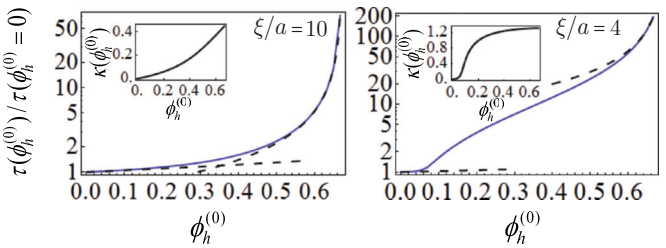

FIG. 3. (Color online) The increase in lifetime due to hybrid lipids, $\tau(\phi_h^{(0)})/\tau(\phi_h^{(0)} = 0)$, for a fluctuation of length scale equal to the fixed correlation length and $\eta = 0.1$. The lifetime associated with that particular length scale is obtained by setting the temperature θ so that the correlation length $\xi/a = 10$ (left panel) or $\xi/a = 4$ (right panel). The dashed lines are limiting expressions valid for small [Eq. (B9)] and large [Eqs. (B10)] $\phi_h^{(0)}$. Inset: The measure of the coupling κ (dimensionless units; see text for definition) between composition and orientation fluctuations increases with increasing hybrid fractions and decreasing fluctuation domain sizes.

as a function of the hybrid fraction at different length scales will be carried out to test (and possibly lead to modification of) the theory.

ACKNOWLEDGMENTS

We are grateful for discussions with Michael Schick, Martin Grant, David Andelman, Shigeyuki Komura, Benjamin Machta, Sarah Veatch, Uri Raviv, James Sethna, Sarah Keller, and Lia Addadi. The Israel Science Foundation, the Schmidt Minerva Center, and the historic generosity of the Perlman Family Foundation are gratefully acknowledged for funding this research. B.P. is grateful to the Azrieli Foundation for support through the award of an Azrieli Fellowship.

APPENDIX A: FLUCTUATION FREE ENERGY, CORRELATION FUNCTION, AND CORRELATION LENGTH

We first recall the mixed phase free energy proposed in Ref. [29],

$$\mathcal{F} = \mathcal{F}_{MF} + \mathcal{F}_{\rm Fluct}, \tag{A1}$$

where

$$\mathcal{F}_{MF} = -2J\left(\phi_s^{(0)} - \phi_u^{(0)}\right)^2 + T\left[\phi_s^{(0)}\ln\left(\phi_s^{(0)}\right) + \phi_u^{(0)}\ln\left(\phi_u^{(0)}\right) + \left(1-\phi_s^{(0)}-\phi_s^{(0)}\right)\ln\left(1-\phi_s^{(0)}-\phi_u^{(0)}\right)\right] \tag{A2}$$

is the mean-field part of the free energy and where $\mathcal{F}_{\rm Fluct}$ is the fluctuation part. The various contributions to $\mathcal{F}_{\rm Fluct}$ defined by Eq. (1) in the main text are given by

$$\mathcal{S} = -\frac{1}{a^2}\int d\mathbf{x}\left\{\frac{1-\phi_u^{(0)}}{2\phi_s^{(0)}\phi_h^{(0)}}\delta\phi_s(\mathbf{x})^2 + \frac{1-\phi_s^{(0)}}{2\phi_u^{(0)}\phi_h^{(0)}}\delta\phi_u(\mathbf{x})^2 + \frac{1}{\phi_h^{(0)}}\delta\phi_s(\mathbf{x})\delta\phi_u(\mathbf{x}) + \frac{1}{\phi_h^{(0)}}|\bar\sigma(\mathbf{x})|^2\right\}, \tag{A3}$$

$$\mathcal{E}_{\phi\phi} = -\frac{2J}{a^2}\int d\mathbf{x}\int d\bar\Delta\; g(\Delta)\Psi(\mathbf{x})\Psi(\mathbf{x}+\bar\Delta), \tag{A4}$$

$$\mathcal{E}_{\phi\sigma} = \frac{2J}{a^2}\int d\mathbf{x}\int d\bar\Delta\; g(\Delta)\hat\Delta\cdot\bar\sigma(\mathbf{x})[\Psi(\mathbf{x}+\bar\Delta)-\Psi(\mathbf{x}-\bar\Delta)], \tag{A5}$$

$$\mathcal{E}^{(1)}_{\sigma\sigma} = \frac{2J}{a^2}\int d\mathbf{x}\int d\bar\Delta\; g(\Delta)[\hat\Delta\cdot\bar\sigma(\mathbf{x})][\hat\Delta\cdot\bar\sigma(\mathbf{x}+\bar\Delta)], \tag{A6}$$

$$\mathcal{E}^{(2)}_{\sigma\sigma} = -\frac{2J}{a^2}\int d\mathbf{x}\int d\bar\Delta\; g(\Delta)[\hat\Delta\times\bar\sigma(\mathbf{x})]\cdot[\hat\Delta\times\bar\sigma(\mathbf{x}+\bar\Delta)], \tag{A7}$$

where a is a nearest-neighbor distance between lipid molecules, J is the unique interaction parameter, and $\Psi(\mathbf{x}) = \delta\phi_s(\mathbf{x}) - \delta\phi_u(\mathbf{x})$. $\delta\phi_s(\mathbf{x})$, $\delta\phi_u(\mathbf{x})$, $\bar\sigma(\mathbf{x})$, $\phi_s^{(0)}$, $\phi_u^{(0)}$, and $\phi_h^{(0)}$ are defined in the main text. There, an approximate expression for $\mathcal{E}_{\sigma\sigma} = \mathcal{E}^{(1)}_{\sigma\sigma} + \mathcal{E}^{(2)}_{\sigma\sigma}$ is reported, rather than for $\mathcal{E}^{(1)}_{\sigma\sigma}$ and $\mathcal{E}^{(2)}_{\sigma\sigma}$ individually. $g(\Delta)$ is a kernel that accounts for the finite range of the interactions. We will use the nearest-neighbor form for $g(\Delta)$ given by

$$g(\Delta) = \frac{1}{2\pi a}\delta(\Delta - a). \tag{A8}$$

The fluctuation part of the free energy [Eq. (2.1)] is conveniently written in a Fourier representation where all the wave-vector fluctuation modes decouple. Using the following definition for the Fourier transform:

$$A(\mathbf{k}) = \frac{1}{2\pi}\int d\mathbf{x}\; e^{-i\mathbf{k}\cdot\mathbf{x}}A(\mathbf{x}), \tag{A9}$$

we obtain an expression for $\mathcal{F}_{\rm Fluct}$ in $\mathbf{k}$ space,

$$\mathcal{F}_{\rm Fluct} = \frac{1}{a^2}\int d\mathbf{k}\;\bar\Psi^T_{-\mathbf{k}}\mathsf{M}_{\mathbf{k}}\bar\Psi_{\mathbf{k}}. \tag{A10}$$

Here, $\bar\Psi_{\mathbf{k}}$ is an array that contains the Fourier components of the composition and orientation fields,

$$\bar\Psi_{\mathbf{k}} = [\delta\phi_s(\mathbf{k}),\delta\phi_u(\mathbf{k}),\sigma_x(\mathbf{k}),\sigma_y(\mathbf{k})], \tag{A11}$$

and the coupling matrix $\mathsf{M}_{\mathbf{k}}$ is given by

$$\mathsf{M}_{\mathbf{k}} = \begin{pmatrix} T\frac{1-\phi_u^{(0)}}{2\phi_s^{(0)}\phi_h^{(0)}} - 2J\mathcal{J}_0(ka) & T\frac{1}{2\phi_h^{(0)}} + 2J\mathcal{J}_0(ka) & -i2J\frac{k_x}{k}\mathcal{J}_1(ka) & -i2J\frac{k_y}{k}\mathcal{J}_1(ka) \\ T\frac{1}{2\phi_h^{(0)}} + 2J\mathcal{J}_0(ka) & T\frac{1-\phi_s^{(0)}}{2\phi_u^{(0)}\phi_h^{(0)}} - 2J\mathcal{J}_0(ka) & i2J\frac{k_x}{k}\mathcal{J}_1(ka) & i2J\frac{k_y}{k}\mathcal{J}_1(ka) \\ i2J\frac{k_x}{k}\mathcal{J}_1(ka) & -i2J\frac{k_x}{k}\mathcal{J}_1(ka) & T\frac{1}{\phi_h^{(0)}} - 2J\frac{k_x^2-k_y^2}{k^2}\mathcal{J}_2(ka) & -4J\frac{k_xk_y}{k^2}\mathcal{J}_2(ka) \\ i2J\frac{k_y}{k}\mathcal{J}_1(ka) & -i2J\frac{k_y}{k}\mathcal{J}_1(ka) & -4J\frac{k_xk_y}{k^2}\mathcal{J}_2(ka) & T\frac{1}{\phi_h^{(0)}} - 2J\frac{k_y^2-k_x^2}{k^2}\mathcal{J}_2(ka) \end{pmatrix}, \tag{A12}$$

where $\mathcal{J}_0$, $\mathcal{J}_1$, and $\mathcal{J}_2$ are the zeroth, first-, and second-order Bessel functions of the first kind.

Any correlation function can be obtained from the following correlation matrix:

$$\left\langle\bar\Psi_{-\mathbf{k}}\bar\Psi^T_{\mathbf{k}'}\right\rangle = \delta_{\mathbf{k}+\mathbf{k}'}\frac{a^2T}{2}\mathsf{M}^{-1}_{\mathbf{k}}. \tag{A13}$$

In particular, the size and shape of saturated-rich fluctuation domains in the mixed phase is characterized by the saturated lipid autocorrelation function,

$$C_{ss}(\mathbf{k}) \equiv \langle\delta\phi_s(-\mathbf{k})\delta\phi_s(\mathbf{k})\rangle = \frac{a^2T}{2}\left[\mathsf{M}^{-1}_{\mathbf{k}}\right]_{11}, \tag{A14}$$

where the subscript 11 means that we refer to the 11 part of the matrix inverse of $\mathsf{M}_{\mathbf{k}}$. In Ref. [29], we showed that $C_{ss}(\mathbf{k})$

is a function of $|\mathbf{k}| = k$ only that is peaked at $k = 0$ below the Lifshitz line $[\phi_h^{(0)} < 2(1-\phi_d^{(0)^2})/3]$. Hence we perform a small k expansion,

$$C_{ss}(k) \approx C_{ss}(k=0) + \frac{1}{2}\frac{\partial^2 C_{ss}(k=0)}{\partial k^2}k^2 \approx \frac{C_{ss}(k=0)}{(1+\xi^2 k^2)}, \tag{A15}$$

where $\xi^2 = -[\partial^2 C_{ss}(k=0)/\partial k^2]/[2C_{ss}(k=0)]$, which determines the width of the correlation function in $\mathbf{k}$ space. That width is related to the real-space decay of the correlation function. Hence, we identify ξ as the correlation length. The resulting expression for ξ is

$$\frac{\xi}{a} = \left\{ \frac{\left(1-\phi_d^{(0)}\right)^2\left(1+\phi_d^{(0)}-\phi_h^{(0)}\right)\left(1-\phi_d^{(0)^2}-\frac{3\phi_h^{(0)}}{2}+\tilde{\theta}\right)}{4\tilde{\theta}\left[1-\phi_d^{(0)}-\phi_h^{(0)}+2\phi_h^{(0)}\phi_d^{(0)}+\left(1-\phi_d^{(0)}+\phi_h^{(0)}\right)\left(\tilde{\theta}-\phi_d^{(0)^2}\right)\right]} \right\}^{1/2}, \tag{A16}$$

where $\tilde{\theta} = (1-\phi_d^{(0)^2}-\phi_h^{(0)})(T-T_S)/T_S$ and where $T_S = 4J(1-\phi_d^{(0)^2}-\phi_h^{(0)})$ is the spinodal temperature. When $\phi_d^{(0)} = 0$, $T_S = T_c$ where T_c is the critical temperature given by Eq. (2.3). Further, when $\theta = (T-T_c)/T_c \to 0$, ξ/a reduces to Eq. (2.4). Figure 4 plots the value of θ for $\phi_d^{(0)} = 0$ and a fixed correlation length (chosen to be $\xi = 10a$ and $\xi = 4a$) as a function of the hybrid lipid fraction. As the amount of hybrid is increased towards the Lifshitz point, the temperature corresponding to small length scale fluctuation domains gets closer to the critical temperature.

Note that Eq. (A16) is only valid if $\phi_h^{(0)} < 2(1-\phi_d^{(0)^2})/3$. Exactly at this value (at the Lifshitz line), higher order terms in the small k expansion must be kept as $\theta \to 0$. In other words, $C_{ss}(k=0) \propto \theta^{-1}$, $\partial^2 C_{ss}(k=0)/\partial k^2 \propto \theta^{-1}$, and $\partial^4 C_{ss}(k=0)/\partial k^4 \propto \theta^{-2}$ as $\theta \to 0$. Hence, at the Lifshitz line, the correlation length is determined by the fourth-order derivative, $\xi^4 \propto -[\partial^4 C_{ss}(k=0)/\partial k^4]/[4!C_{ss}(k=0)]$. The result is that the correlation length diverges like $\theta^{-1/4}$ as $\theta \to 0$, as stated in the main text.

APPENDIX B: FLUCTUATION LIFETIME: FOURIER REPRESENTATION

The dynamics are conveniently written in the Fourier representation of the fluctuations described in Appendix A.

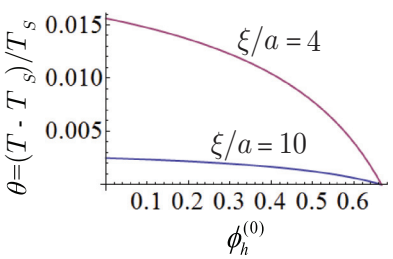

FIG. 4. (Color online) The temperature, $\theta = (T-T_c)/T_c$, at which the correlation length is $\xi = 10a$ (blue, bottom curve) and $\xi = 4a$ (magenta, top curve) as a function of the hybrid lipid fraction.

In that representation, Eqs. (2.5) and (2.6) are written as

$$\frac{\partial \bar{\Psi}_{\mathbf{k}}(t)}{\partial t} = -\frac{2D_0}{a^4}\Lambda_{\mathbf{k}}\mathsf{M}_{\mathbf{k}}\bar{\Psi}_{\mathbf{k}}(t), \tag{B1}$$

where $\Lambda_{\mathbf{k}}$ is a diagonal matrix that contains the dynamical coefficients,

$$\Lambda_{\mathbf{k}} = \mathrm{diag}[(ak)^2,(ak)^2,\eta,\eta], \tag{B2}$$

where $\eta = a^2\Gamma/D_0$ is the ratio of the time scale for a lipid to diffuse one molecular size over the reorientation time scale. D_0 is related to the lipid diffusion coefficient, D ($D_0 = a^2 D/T$,) while Γ is related to the inverse orientation relaxation time scale, γ ($\Gamma = a^2\gamma/T$). Values for D, γ, and a are reported in the main text and they give $\eta \approx 1$. Note that D_0 and Γ are assumed to be independent of temperature so that D and γ depend on T linearly. Hence, the temperature that relates D_0 with D (and Γ with γ) is the temperature at which the experimental determination of D (γ) was performed. Here, we assume that this temperature can be written as $T = \alpha J$ where α is a proportionality factor of the order of one. For the ratio of lifetimes reported in the main text (with and without hybrids), this parameter is irrelevant. Hence, we will set $\alpha = 1$ for the remainder of the calculation. We can finally write

$$\frac{\partial \bar{\Psi}_{\mathbf{k}}(t)}{\partial t} = -\frac{2D}{a^2}\mathcal{T}_{\mathbf{k}}^{-1}\bar{\Psi}_{\mathbf{k}}(t), \tag{B3}$$

where $\mathcal{T}_{\mathbf{k}}^{-1} = \Lambda_{\mathbf{k}}\mathsf{M}_{\mathbf{k}}/J$.

The decay rate of any fluctuation can be obtained from the matrix $\mathcal{T}_{\mathbf{k}}^{-1}$. The eigenvalues $\nu_{\mathbf{k}}$ of $\mathcal{T}_{\mathbf{k}}^{-1}$ are inversely proportional to the fluctuation lifetimes, $\tau(\mathbf{k}) = a^2\nu_{\mathbf{k}}^{-1}/2D$. The corresponding eigenvectors $\bar{V}_{\mathbf{k}}$ determine the relative amplitudes of the fluctuation components $[\delta\phi_s(\mathbf{k})$, $\delta\phi_u(\mathbf{k})$, $\sigma_x(\mathbf{k})$ and $\sigma_y(\mathbf{k})]$ for a mode that decays on a time scale $\tau(\mathbf{k})$. To get the lifetime of fluctuations of length scale λ such as the one given by Eq. (2.7), we need to choose the magnitude of $\mathbf{k}$ to be $k = 2\pi/\lambda$. The fact that the system is rotationally invariant allows us to arbitrarily set $k_x = 2\pi/\lambda$ and $k_y = 0$ with no loss of generality. With this choice, $\mathcal{T}_{\mathbf{k}}^{-1}$

becomes

$$\mathcal{T}_\lambda^{-1}=\begin{pmatrix} \frac{8\pi^2a^2}{\lambda^2\phi_h^{(0)}}\left[\theta^+-\phi_h^{(0)}\mathcal{J}_0(2\pi a/\lambda)\right] & \frac{8\pi^2a^2}{\lambda^2\phi_h^{(0)}}\left[\theta^-+\phi_h^{(0)}\mathcal{J}_0(2\pi a/\lambda)\right] & -i\frac{8\pi^2a^2}{\lambda^2}\mathcal{J}_1(2\pi a/\lambda) & 0 \\ \frac{8\pi^2a^2}{\lambda^2\phi_h^{(0)}}\left[\theta^-+\phi_h^{(0)}\mathcal{J}_0(2\pi a/\lambda)\right] & \frac{8\pi^2a^2}{\lambda^2\phi_h^{(0)}}\left[\theta^+-\phi_h^{(0)}\mathcal{J}_0(2\pi a/\lambda)\right] & -i\frac{8\pi^2a^2}{\lambda^2}\mathcal{J}_1(2\pi a/\lambda) & 0 \\ i2\eta\mathcal{J}_1(2\pi a/\lambda) & -i2\eta\mathcal{J}_1(2\pi a/\lambda) & \frac{2\eta}{\phi_h^{(0)}}\left[2\theta^--\phi_h^{(0)}\mathcal{J}_2(2\pi a/\lambda)\right] & 0 \\ 0 & 0 & 0 & \frac{2\eta}{\phi_h^{(0)}}\left[2\theta^-+\phi_h^{(0)}\mathcal{J}_2(2\pi a/\lambda)\right] \end{pmatrix},$$

where $\theta^+=(1+\phi_h^{(0)})(1+\theta)$ and $\theta^-=(1-\phi_h^{(0)})(1+\theta)$. The simple structure of this matrix allows one to obtain the eigenvalues and eigenvectors analytically. In the following and in the analysis presented in the main text, we assume that the lifetime of the fluctuation given by Eq. (7) is determined by the smallest eigenvalue, $\nu_{\lambda,\min}$, alone. Accordingly, the fluctuation amplitudes $\bar{\Psi}^{(a,b)}$ are determined by the eigenvector, $\bar{V}_{\lambda,\min}$, corresponding to that eigenvalue. This approximation is accurate as long as there is a large difference in the magnitude of the eigenvalues (i.e., when one is much smaller than all others). We have checked that the smallest eigenvalue is at least tenfold smaller than the others in the regime of interest ($\theta \ll 1$, $\phi_h^{(0)} < 2/3$, and $\eta \approx 1$). Under these conditions, the minimum eigenvalue is given by

$$\nu_{\lambda,\min}=\frac{g+\eta f}{\phi_h^{(0)}}-\frac{1}{\phi_h^{(0)}}\left[(g-\eta f)^2+\frac{32\eta\pi^2a^2\phi_h^{(0)2}}{\lambda^2}\mathcal{J}_1(2\pi a/\lambda)^2\right]^{1/2}, \tag{B4}$$

where

$$f=2\big(1-\phi_h^{(0)}\big)(1+\theta)-\phi_h^{(0)}\mathcal{J}_2(2\pi a/\lambda) \tag{B5}$$

and

$$g=\frac{8\pi^2a^2}{\lambda^2}\phi_h^{(0)}[1+\theta-\mathcal{J}_0(2\pi a/\lambda)]. \tag{B6}$$

Equation (B4) was used to plot $\tau(\theta,\phi_h^{(0)})=a^2\nu_{\lambda,\min}^{-1}/2D$ in Fig. 2. Expanding Eq. (B4) around $\theta=0$ and $\lambda^{-1}=0$ results in Eq. (2.8) reported in the main text. The eigenvector associated with the smallest eigenvalue, $\bar{V}_{\lambda,\min}$, can also obtained analytically,

$$\bar{V}_{\lambda,\min}=(-h,h,i,0)^T, \tag{B7}$$

where

$$h=\frac{4\pi^2a^2}{\lambda^2\phi_h^{(0)}}\times\left(\frac{2\eta\phi_h^{(0)2}\mathcal{J}_1(2\pi a/\lambda)^2-\left[\big(1-\phi_h^{(0)}\big)(1+\theta)+\phi_h^{(0)}\mathcal{J}_0(2\pi a/\lambda)\right]\left\{g-\eta f-\left[(g-\eta f)^2+\frac{32\eta\pi^2a^2\phi_h^{(0)}}{\lambda^2}\mathcal{J}_1(2\pi a/\lambda)^2\right]^{1/2}\right\}}{\eta\mathcal{J}_1(2\pi a/\lambda)\left\{\frac{16\pi^2a^2}{\lambda^2}(1+\theta)-(g+\eta f)+\left[(g-\eta f)^2+\frac{32\eta\pi^2a^2\phi_h^{(0)}}{\lambda^2}\mathcal{J}_1(2\pi a/\lambda)^2\right]^{1/2}\right\}}\right). \tag{B8}$$

Note that the second smallest eigenvalue is usually associated with the eigenvector $\bar{V}_\lambda=(0,0,0,1)^T$ and, hence, is not relevant to the composition fluctuations; it describes the fluctuation of σ_y decoupled from everything else.

For the special case where the fluctuation length scale matches the correlation length, λ is set to ξ in Eq. (2.7) where θ is written in terms of ξ and $\phi_h^{(0)}$ by inverting Eq. (A16) for $\phi_d^{(0)}=0$. The resulting expressions for the smallest eigenvalues, $\nu_{\lambda=\xi,\min}$, and the corresponding eigenvector, $\bar{V}_{\lambda=\xi,\min}$, were used to generate Fig. 3. Here, for simplicity, we report approximate expressions for the eigenvalues only and that are valid for important limiting cases. The results are

$$\nu_{\lambda=\xi,\min}=\frac{4\pi^2a^4}{\xi^4}\{1+4(\xi^2/a^2)[1-\mathcal{J}_0(2\pi a/\xi)]\}-\phi_h^{(0)}\frac{4\pi^2a^4}{\xi^4[1+4(\xi^2/a^2)]}\{1+2(\xi^2/a^2)[1+4(\xi^2/a^2)\mathcal{J}_1(2\pi a/\xi)^2]\}, \tag{B9}$$

valid for small hybrid fraction, $\phi_h^{(0)} \ll 1$, and

$$\begin{aligned}\nu_{\lambda=\xi,\min}=&\frac{8\pi^2a^2}{\xi^2}[1-\mathcal{J}_0(2\pi a/\xi)]+\eta[1-\mathcal{J}_2(2\pi a/\xi)]\\&-\left(\frac{32\eta\pi^2a^2\mathcal{J}_1(2\pi a/\xi)^2}{\xi^2}+\left\{\frac{8\pi^2a^2}{\xi^2}[1-\mathcal{J}_0(2\pi a/\xi)]-\eta[1-\mathcal{J}_2(2\pi a/\xi)]\right\}^2\right)^{1/2}\\&+\frac{3\xi^2\big(2-3\phi_h^{(0)}\big)}{4\xi^2-a^2}\left\{\left(2\eta+\frac{4\pi^2a^4}{\xi^4}\right)+\frac{\big(2\eta-\frac{4\pi^2a^4}{\xi^4}\big)\left\{\frac{8\pi^2a^2}{\xi^2}[1-\mathcal{J}_0(2\pi a/\xi)]-\eta[1-\mathcal{J}_2(2\pi a/\xi)]\right\}}{\left(\frac{32\eta\pi^2a^2\mathcal{J}_1(2\pi a/\xi)^2}{\xi^2}+\left\{\frac{8\pi^2a^2}{\xi^2}[1-\mathcal{J}_0(2\pi a/\xi)]-\eta[1-\mathcal{J}_2(2\pi a/\xi)]\right\}^2\right)^{1/2}}\right\},\end{aligned} \tag{B10}$$

valid for $0 < 2/3-\phi_h^{(0)} \ll 1$. These approximate expressions were used to generate the dashed lines in Fig. 3.

[1] S. Mayor and M. Rao, Traffic **5**, 231 (2004).
[2] J. Hancock and R. Parton, Biochem. J. **389**, 1 (2005).
[3] K. Suzuki, T. Fujiwara, F. Sanematsu, R. Iino, M. Edidin, and A. Kusumi, J. Cell. Biol. **177**, 717 (2007).
[4] S. Chiang, C. Baumann, M. Kanzaki, D. Thurmond, R. Watson, C. Neudauer, I. Macara, J. Pessin, and A. Saltiel, Nature (London) **410**, 944 (2001).
[5] N. Suzuki, S. Suzuki, D. Millar, M. Unno, H. Hara, T. Calzascia, S. Yamasaki, T. Yokosuka, N. Chen, A. Elford *et al.*, Science **311**, 1927 (2006).
[6] A. Palazzo, C. Eng, D. Schlaepfer, E. Marcantonio, and G. Gundersen, Science **303**, 836 (2004).
[7] H. Kamiguchi, J. Neurochem. **98**, 330 (2006).
[8] E. Takahashi, O. Inanami, T. Ohta, A. Matsuda, and M. Kuwabara, Leuk. Res. **30**, 1555 (2006).
[9] C. Hattori, M. Asai, H. Onishi, N. Sasagawa, Y. Hashimoto, T. Saido, K. Maruyama, S. Mizutani, and S. Ishiura, J. Neurosci. Res. **84**, 912 (2006).
[10] C. Dietrich, L. Bagatolli, Z. Volovyk, N. Thompson, M. Levi, K. Jacobson, and E. Gratton, Biophys. J. **80**, 1417 (2001).
[11] A. V. Samsonov, I. Mihalyov, and F. S. Cohen, Biophys. J. **81**, 1486 (2001).
[12] S. L. Veatch and S. L. Keller, Phys. Rev. Lett. **89**, 268101 (2002).
[13] G. W. Feigenson and J. Buboltz, Biophys. J. **80**, 2775 (2001).
[14] F. Heberle, J. Wu, S. Goh, R. Petruzielo, and G. Feigenson, Biophys. J. **99**, 3309 (2010).
[15] T. Konyakhina, S. Goh, J. Amazon, F. Heberle, J. Wu, and G. Feigenson, Biophys. J. **101**, L08 (2011).
[16] G. van den Bogaart, K. Meyenberg, H. Risselada, H. Amin, K. Willig, B. Hubrich, M. Dier, S. Hell, H. Grubmüller, U. Diederichsen *et al.* , Nature (London) **479**, 552 (2011).
[17] S. Veatch, P. Cicuta, P. Sengupta, A. Honerkamp-Smith, D. Holowka, and B. Baird, ACS Chem. Biol. **5**, 287 (2008).
[18] I. Levantal, M. Grzybek, and K. Simons, Proc. Natl. Acad. Sci. USA **108**, 11411 (2011).
[19] N. Goldenfeld, *Lectures on Phase Transitions and the Renormalization Group* (Perseus, Reading, MA, 1992).
[20] P. Hohenberg and B. Halperin, Rev. Mod. Phys. **49**, 435 (1977).
[21] A. R. Honerkamp-Smith, B. B. Machta, and S. L. Keller, Phys. Rev. Lett. **108**, 265702 (2012).
[22] J. Hancock, Nat. Rev. Mol. Cell Biol. **7**, 456 (2006).
[23] W. K. Subczynski and A. Kusumi, Biochim. Biophys. Acta **1610**, 231 (2003).
[24] S. Ramachandran, S. Komura, K. Sekib, and M. Imaic, Soft Matter **7**, 1524 (2011).
[25] B. Machta, S. Papanikolaou, J. Sethna, and S. Veatch, Biophys. J. **100**, 1668 (2011).
[26] A. Yethiraj and J. Weisshaar, Biophys. J. **93**, 3113 (2007).
[27] T. Fischer, H. Risseladab, and R. Vink, Phys. Chem. Chem. Phys. **14**, 14500 (2012).
[28] T. Witkowski, R. Backofena, and A. Voigt, Phys. Chem. Chem. Phys. **14**, 14509 (2012).
[29] B. Palmieri and S. A. Safran, Langmuir **29**, 5246 (2013).
[30] S. Trabelsi, S. Zhang, T. R. Lee, and D. K. Schwartz, Phys. Rev. Lett. **100**, 037802 (2008).
[31] O. Szekely, Y. Schilt, A. Steiner, and U. Raviv, Langmuir **27**, 14767 (2011).
[32] F. A. Heberle, R. S. Petruzielo, J. Pan, P. Drazba, N. Kučerka, R. F. Standaert, G. W. Feigenson, and J. Katsaras, J. Am. Chem. Soc. **135**, 6853 (2013).
[33] T. Galimzyanov and S. Akimov, JETP Lett. **93**, 463 (2011).
[34] M. Schick, Phys. Rev. E **85**, 031902 (2012).
[35] T. Galimzyanov, R. Molotkovsky, B. Kheyfets, and S. Akimov, JETP Lett. **96**, 681 (2012).
[36] S. Meinhardt, R. Vink, and F. Schmid, Proc. Natl. Acad. Sci. USA **110**, 4476 (2013).
[37] M. W. Matsen and D. E. Sullivan, Phys. Rev. A **41**, 2021 (1990).
[38] Y. Hirose, S. Komura, and D. Andelman, Phys. Rev. E **86**, 021916 (2012).
[39] M. Teubner and R. Strey, J. Chem. Phys. **87**, 3195 (1987).
[40] G. Gompper and M. Schick, Phys. Rev. Lett. **65**, 1116 (1990).
[41] R. Brewster, P. Pincus, and S. Safran, Biophys. J. **97**, 1087 (2009).
[42] T. Yamamoto, R. Brewster, and S. Safran, Europhys. Lett. **91**, 28002 (2010).
[43] T. Yamamoto and S. Safran, Soft Matter **7**, 7021 (2011).
[44] P. Chaikin and T. Lubensky, *Principles of Condensed Matter Physics* (Cambridge University Press, Cambridge, 1995).
[45] A. Honigmann, C. Walter, F. Erdmann, C. Eggeling, and R. Wagner, Biophys. J. **90**, 2886 (2010).
[46] R. Austin, S. Chan, and T. Jovin, Proc. Natl. Acad. Sci. USA **76**, 5650 (1979).
[47] J. Korlach, P. Schwille, W. W. Webb, and G. W. Feigenson, Proc. Natl. Acad. Sci. USA **96**, 8461 (1999).
[48] L. Davenport and P. Targowski, Biophys. J. **71**, 1837 (1996).
[49] C. Rosetti and C. Pastorino, J. Phys. Chem. B **111**, 3525 (2012).
[50] K. Inaura and Y. Fujitani, J. Phys. Soc. Jpn. **77**, 114603 (2008).
[51] M. Haataja, Phys. Rev. E **80**, 020902(R) (2009).